RESEARCH ARTICLE

Remains of the 19th Century: Deep storage of contaminated hydraulic mining sediment along the Lower Yuba River, California

Tyler K. Nakamura[*], Michael Bliss Singer[†,‡] and Emmanuel J. Gabet[*]

Since the onset of hydraulic gold mining in California's Sierra Nevada foothills in 1852, the environmental damage caused by displacement and storage of hydraulic mining sediment (HMS) has been a significant ecological problem downstream. Large volumes of mercury-laden HMS from the Yuba River watershed were deposited within the river corridor, creating the anthropogenic Yuba Fan. However, there are outstanding uncertainties about how much HMS is still contained within this fan. To quantify the deep storage of HMS in the Yuba Fan, we analyzed mercury concentrations of sediment samples collected from borings and outcrops at multiple depths. The mercury concentrations served as chemostratigraphic markers to identify the contacts between the HMS and underlying pre-mining deposits. The HMS had mercury concentrations at least ten-fold higher than pre-mining deposits. Analysis of the lower Yuba Fan's volume suggests that approximately 8.1×10^7 m³ of HMS was deposited within the study area between 1852 and 1999, representing ~32% of the original Yuba Fan delivered by 19th Century hydraulic gold mining. Our estimate of the mercury mass contained within this region is 6.7×10^3 kg, which is several orders of magnitude smaller than what was estimated to have been lost to the mining process. We suggest that this discrepancy is likely due to a combination of missing (yet to be found) mercury masses stored upstream, overestimated losses during mining, and high delivery of mercury to the lowland Sacramento Valley and to the San Francisco Bay-Delta system, where it poses a great risk to sensitive ecosystems.

Keywords: Mercury; Ecosystems; Sediment transport; Geomorphology; Alluvial fan; Bay-Delta

Introduction

Large-scale hydraulic mining operations in the Sierra Nevada of Northern California began in 1852 with the invention of the hydraulic monitor, a high-pressure water cannon, and lasted until the Sawyer Decision halted hydraulic mining in 1884 (Alpers and Hunerlach, 2000). The hydraulic mines in the northern Sierra Nevada operating during this period used hydraulic monitors with water delivered from higher elevations to generate high hydraulic head (pressure) capable of removing overburden to access the underlying Tertiary auriferous (gold-bearing) gravel deposits (Yeend, 1974; Lindgren, 1911). The slurry of water and eroded sediment produced from hydraulic mining was diverted into systems of sluice-boxes where gold was removed from the unconsolidated mixture of gravel and sands via gravity separation. Mercury was

added to the sluice-boxes so that it would alloy with the gold, forming an amalgam that increased the weight of the gold for easier recovery. The amalgam was then roasted to release mercury as a vapor and isolate the gold (Averill, 1946). Approximately 1.2×10^7 kg of mercury mined from the Coast Ranges were used in mining operations within the Sierra Nevada during the mid to late 1800s (Alpers and Hunerlach, 2000).

Mercury was lost to the environment during the process of recovering gold from the Tertiary gravels within the sluice-boxes. The amount of mercury lost from the sluice-boxes depended on the quantity of water used, sluice slope, sluice length, and the presence of leaks (Bowie, 1893). Averill (1946) investigated hydraulic mines operating in the 1930s (decades after the active Sierra Nevada mining period) and implied that approximately 10–30% of mercury was lost from the sluices to the environment. The majority of the mines in the Sierra Nevada washed hydraulic mining sediment (HMS) and waste left over from the amalgamation process into nearby creeks and rivers (Hunerlach et al., 1999). This HMS was contaminated by mercury from the amalgamation process, and it became susceptible to further downstream transport (Bowie, 1893).

[*] Geology Department, San Jose State University, San Jose, California, US

[†] School of Earth and Ocean Sciences, Cardiff University, Cardiff, Wales, UK

[‡] Earth Research Institute, University of California Santa Barbara, Santa Barbara, California, US

Corresponding author: Michael Bliss Singer (bliss@eri.ucsb.edu)

Geomorphic changes within HMS deposits downstream of Sierra Nevada mines have been significant since the onset of hydraulic mining, including sediment erosion, redistribution, and export of HMS to lowland environments (Gilbert, 1917; James, 1989; James, 1991; James et al., 2009; Ghoshal et al., 2010; Kilham et al., 2012; Singer et al., 2013; Higson and Singer, 2015). The large amount of sedimentation in lowland waters exacerbated flooding, altered the course of the rivers, and disrupted agricultural operations (Gilbert, 1917; James, 2005; Kelley, 1998; Singer et al., 2008). In 1884, due to damage associated with the mines, Judge Lorenzo Sawyer issued an injunction against the mining operations to discontinue hydraulic mining operations (James, 2005). The Caminetti Act of 1893 legalized hydraulic mining with the provision that mining tailings must be prevented from reaching adjacent streams (James, 2005). Under the Caminetti Act, the California Debris Commission (CDC) inspected sediment detention structures and issued licenses for specific volumes of sediment releases. Between 1893 and 1950, mercury continued to be used to extract gold from the mining sediment within the Yuba River watershed (James, 2005). The mercury-rich sediment from these later operations was stored near the mines, and the geomorphic impacts to downstream environments were far less significant compared to that from the HMS produced between 1853 and 1884.

The Yuba River basin (**Figure 1**) was the 'epicenter' of Sierra Nevada hydraulic mining and thus received a massive amount of sediment that coalesced into a large anthropogenic fan (Singer et al., 2013). G.K. Gilbert was commissioned by the CDC in the early 1900s to study the impact of mining on downstream water courses. Gilbert (1917) estimated that 5.23×10^8 m^3 of HMS were produced within the mines along the Yuba River between 1849 and 1908. Gilbert's field work revealed that a large

fan deposit of HMS had accumulated over ~40 km of river length from the river canyon in the Sierra Nevada foothills to the mouth of the Yuba River at Marysville, and he estimated that the volume of the Yuba Fan deposit was approximately 2.52×10^8 m^3. The lower Yuba Fan consists of HMS that has accumulated along the Yuba River from the confluence of the Feather River to the Yuba Goldfields (**Figures 1** and **2**) and within the confines of levees built during the 1880s (James et al., 2009).

In recent decades, the mercury-laden HMS introduced to the Yuba River and other watersheds throughout the Sierra Nevada and Central Valley has been a significant contamination concern due to the potential harm that mercury can cause to ecosystems and to humans that consume local fish. The inorganic mercury adsorbed to HMS can be converted to neurotoxic monomethylmercury (MMHg) by sulfate-reducing or iron-reducing microbes operating at the sediment-water interface (Gilmour et al., 2013). In this form, mercury can be easily taken up by the biota and then pass through the blood-brain barrier in animals, creating developmental problems, deformities, and other acute health problems (Mergler et al., 2007; Cristol et al., 2008). There is a large body of evidence that mercury delivered to rivers and streams in the Sierra Nevada foothills during the 19th century has been converted to MMHg and is subsequently being taken up by aquatic migratory biota including algae, aquatic insects, bivalves, forage fish, salmonids, sportfish, and waterfowl throughout the geographical region downstream of hydraulic mining sites (Heim et al., 2007; Davis et al., 2008; Wiener and Suchanek, 2008; Henery et al., 2010; Windham-Myers et al., 2014; Donovan et al., 2016a). Mercury isotope analyses performed by Donovan et al. (2016b) suggest that MMHg contamination of food webs within the Yuba River watershed is associated with the HMS, which corroborates a previous isotopic study in the Bay-Delta (Gehrke et al.,
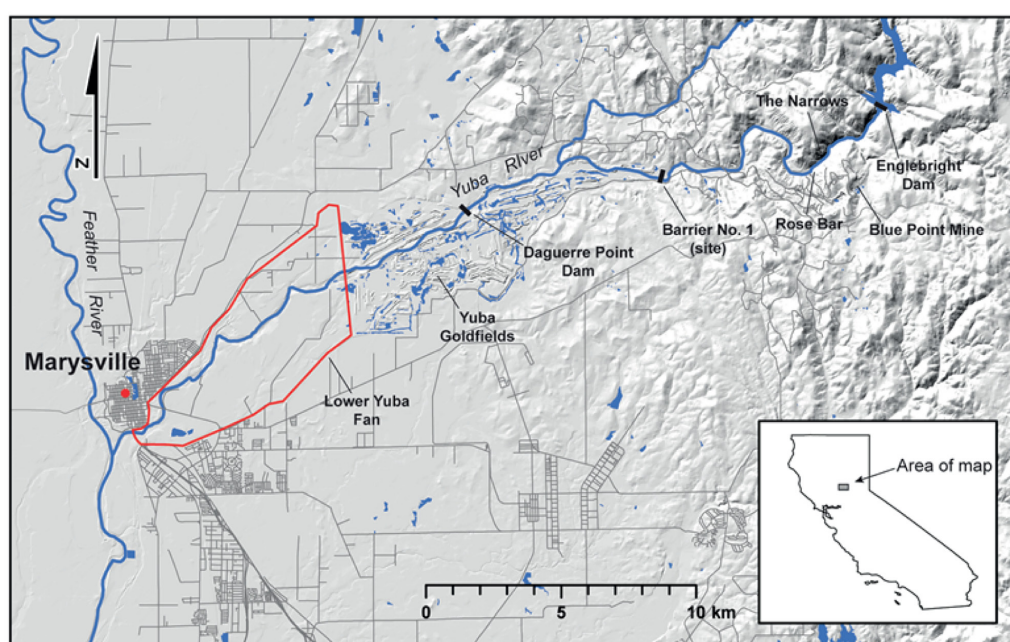

Figure 1: Lower Yuba River between Marysville, CA, and Englebright Dam. The red polygon near Marysville, CA, outlines the lower Yuba Fan. The base map is a digital elevation model from the U.S. Geological Survey (2013). DOI: https://doi.org/10.1525/elementa.333.f1
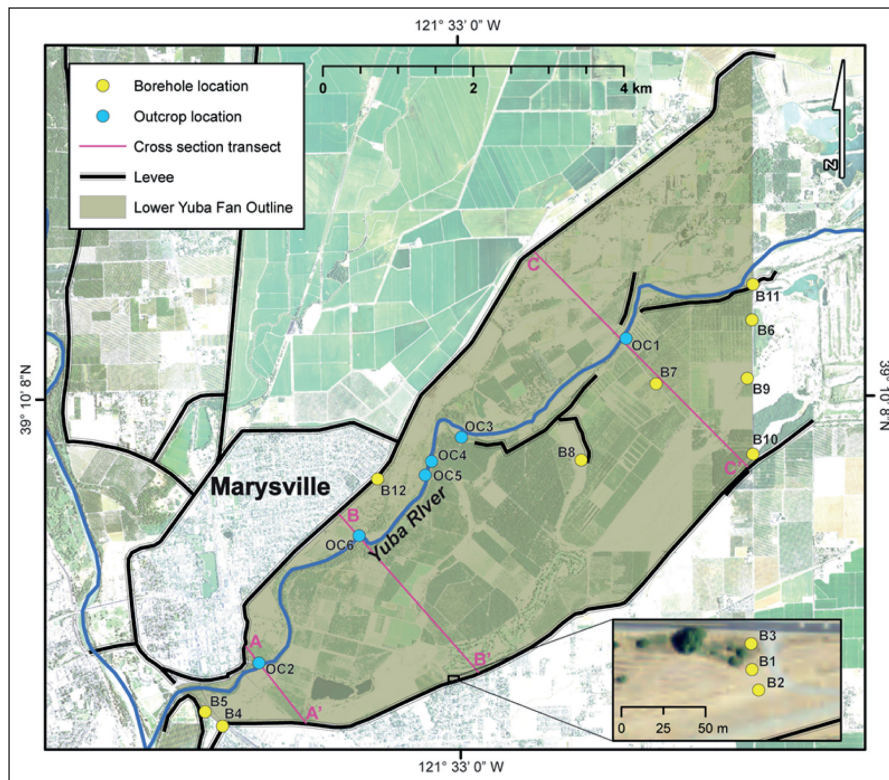
Figure 2: Lower Yuba Fan study area. The map includes sampling locations and cross section transects. The base map is aerial orthoimagery from the USDA (2014a, 2014b, 2014c, 2014d, 2014e, and 2014f). DOI: https://doi.org/10.1525/elementa.333.f2

2011). Singer et al. (2016) demonstrated through hydraulic modeling and MMHg production potential calculations that widespread bioaccumulation of MMHg through the food web of the Yuba River likely occurs within floodplains of the lower Yuba River as the HMS becomes inundated during floods, and this mercury is also transported into ecologically sensitive lowland environments.

In this context, 19ᵗʰ Century HMS stored along the Yuba River can be conceived of as a reservoir of toxicity to local migratory food webs, with potentially adverse consequences for the broader Bay-Delta region. Sediment is the link between upland and lowland ecosystems since contaminated HMS can be eroded from storage during large floods that occur approximately once a decade, and then transported downstream into the lowland Central Valley to eventually reach San Francisco Bay-Delta (Singer et al., 2013). Therefore, understanding the geomorphic history of sediment erosion and deposition along major rivers of the Sierra Nevada is a fundamental aspect of mercury pollution in the Central Valley and San Francisco Bay-Delta. Although previous research demonstrated that HMS with adsorbed mercury reaches the lowlands (Singer et al., 2013; Bouse et al., 2010; Killham et al., 2012), the extent to which major anthropogenic fans, such as the Yuba Fan, retain HMS and its associated mercury is unknown. This study builds on previous geomorphic research (James, 1989; James, 1997; James, 2004; James et al., 2009; Ghoshal et al., 2010) documenting sustained storage of mining sediment along Sierra Nevada streams over different time periods (Springborn et al., 2011). Our work combines DEM differencing of the Yuba Fan surface over various time periods, deep coring, and chemostratigraphy

within Yuba Fan deposits to document the Yuba Fan HMS in 3 dimensions. Our results, therefore, provide an improved estimate of total HMS and mercury storage within the lower Yuba Fan that can illuminate the scale of the regional environmental problem, as the Sacramento Valley continues to grapple with the contamination legacy of 19ᵗʰ Century hydraulic gold mining in the Sierra Nevada.

Materials and Methods
Sampling techniques
Sediment samples were collected from borings and outcrops along the lower Yuba Fan. Boring samples were manually obtained using a stainless steel closed bucket, which was 8.5 cm in diameter and 18.5 cm long, attached to a hand auger. The closed cylinder prevents the sample from becoming contaminated with surrounding material within the bore hole. During augering, samples with a minimum mass of 1 kg were collected at approximately 1-m depth intervals in each boring. To characterize likely changes in sediment sources, additional samples were taken when sedimentological changes were detected in the boring spoils. At depths greater than 6 m, sampling by auger was inefficient because the length of the extension rods made it difficult to retain the sediment within the auger bucket when extracting the sample from the borehole. Therefore, the maximum possible augering depth was approximately 6 m. Significant changes in sediment type or color were used as indicators of whether the pre-mining sediment was encountered. Each borehole was augered until pre-mining deposits were reached or the maximum possible depth was attained. The vertical accuracy of the contact depths was ±0.50 m.

The stratigraphic outcrops along the Yuba River that were surveyed and sampled consisted of cut banks along the river channel. Outcrop thickness was measured with a stadia rod and hand level. Changes in sediment type and color were documented in the field.

Site selection

Sediment samples from 11 boreholes were collected within the lower Yuba Fan between the Yuba River and flood control levees that bound the river corridor; six of the boreholes were located close to the levees (**Figure 2**). Samples were not collected from borehole B9 because the sediment at the site was too coarse to retain the samples in the auger bucket. To augment the information from the borings, six outcrops were surveyed and sampled along the Yuba River at cut-bank locations (**Figure 2**).

Sediment samples were also collected upstream of the lower Yuba Fan at the Blue Point Mine and Rose Bar in order to characterize the mercury concentrations of end-member samples (**Figure 3**). The Blue Point Mine exposes *in situ* auriferous gravels; 6 samples from this site were analyzed for mercury content to reveal the background concentrations of the auriferous gravels within the study area, prior to Hg addition. Rose Bar comprises a large terrace of mine tailings associated with the Blue Point Mine (Higson and Singer, 2015), so it contains high Hg concentrations associated with active mining (Singer et al., 2013). Seven samples were collected from Rose Bar in order to determine the mercury concentration of 'primary' HMS before being reworked by the Yuba River. We specifically avoided the middle part of the Yuba Fan,

which is within a zone called Yuba Gold Fields, where dredger mining has dramatically altered the landscape and affected the sediment and chemostratigraphy.

Particle size distribution

The particle size distribution of the sediments can provide valuable information about the potential for mercury contamination and the downstream transport of HMS. Sediment size distributions were obtained using a laboratory test sieve vibrator and Micrometrics SediGraph 5100 Particle Size Analyzer. The following grain sizes were investigated: greater than 2 mm (gravel), 2 mm to 62.5 μm (sand), 62.5 μm to 4 μm (silt), and smaller than 4 μm (clay). The moderately to well indurated soils could not be dry-sieved properly due to low friability. For these samples, we performed a wet-sieve analysis to measure the fine-grained fraction of the sample using a 63 μm sieve. The material caught on the sieve was dried, and a dry-sieve analysis was performed. The sediment that passed through the 63 μm sieve was analyzed using the Sedigraph to determine the distribution of silt and clay in each sample.

Mercury concentration analysis

Fine-grained fractions of the samples (<63 μm) were also obtained for mercury analysis with stainless steel sieves washed with isopropyl alcohol and deionized water between samples to prevent cross-contamination. The fine-grained samples were analyzed for total mercury in the USGS Mercury Lab at Menlo Park, CA on a Tekran Cold Vapor Atomic Fluorescence System (CVAFS), under the auspices of Dr. Mark Marvin-Pasquale, using the EPA
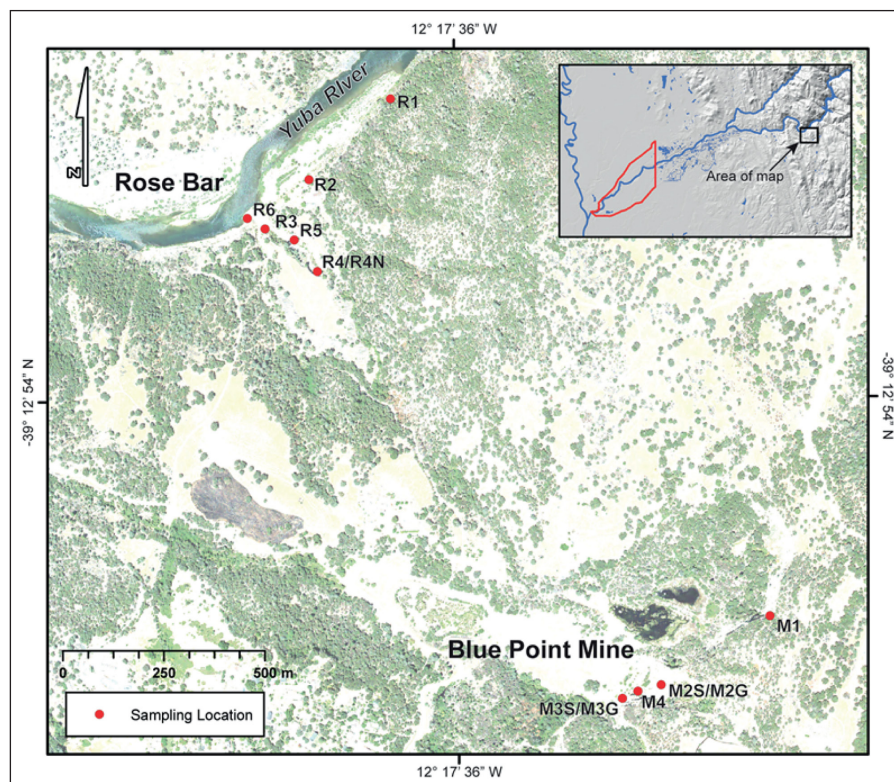

Figure 3: Sampling locations at Blue Point Mine and Rose Bar. The base map is aerial orthoimagery from the USDA (2014g). DOI: https://doi.org/10.1525/elementa.333.f3

Method 1631 for solids preparation and analysis for total mercury via cold vapor atomic fluorescence mass spectrometer (Olund et al., 2005). The minimum mercury concentrations that can be detected range from 0.6×10^{-3} ppm to 0.6×10^{-2} ppm.

Chemostratigraphy analysis

Singer et al. (2013) found that the contact between the pre-mining deposits and the HMS within stratigraphic sections could be identified by an order of magnitude increase in total mercury concentration in the fine-grained fraction of the sediment above a background concentration <0.08 µg/g, which corroborates other work in the Sacramento Valley (Bouse et al., 2010). Therefore, the contact between the pre-mining deposits and HMS was located within the borings and stratigraphic columns by identifying areas that had abrupt order-of-magnitude changes in mercury concentration. These contact depths were used to model the spatially contiguous pre-mining surface using GIS.

Geographic information systems analysis

The pre-mining surface of the lower Yuba Fan was modeled using ArcGIS 10.4.1 (Environmental Systems Research Institute, 2013). The modern ground surface elevation was found for each site using a 1-m digital elevation model (DEM) from 1999 vertical accuracy of the DEM is ±0.15 m (Stonestreet and Lee, 2000). The elevation of the pre-mining surface at each field location was determined by subtracting the depth of the contact between the pre-mining surface and the HMS from the modern surface elevation. Although HMS at first spread out to form the Yuba Fan across a wide swath of the valley, the extent of the deposits was restricted by levees built along the northern side of the Yuba River in the 1880s (James et al., 2009). Therefore, elevations along the base of the northern levee were identified from the 1999 DEM and were used to recreate the 1852 surface. The elevation data were interpolated using the 'topo to raster' tool in ArcGIS, which creates a hydrologically accurate drainage structure while eliminating the presence of large sinks (Hutchinson, 1989), to create a 1-m resolution DEM representing the pre-mining surface.

Digital topographic maps obtained from the USGS were used to create DEMs of the lower Yuba Fan for the years 1911 and 1952 (U.S. Geological Survey, 1911; U.S. Geological Survey, 1952). The vertical accuracy of the topographic maps is ±0.76 m (U.S. Geological Survey, 1999). These maps were georeferenced in ArcGIS via using the georeferencing interactive toolset. Multipoint shapefiles were created, each containing thousands of point features located along the contour lines. Each point feature was assigned an elevation that corresponded to the contour line on which it was placed. The shapefiles were converted into 1-m resolution raster surfaces using inverse distance weighted (IDW) interpolation, which predicts the elevation of each raster cell within the model grid using surrounding known elevation values.

All DEMs (pre-mining surface, 1911, 1952 and 1999) were compared sequentially using the 'minus' operation of raster algebra, which subtracts the cell elevations

of the most recent DEM from the cell elevations of the older DEM, to create maps showing the areas and magnitudes of elevation changes. Cross sections were generated from the DEMs using the 'stack profile' tool. We used the cut-and-fill operation, which determines the changes in material volume by using the difference in elevation and the area of each cell, to determine the amount of material that had been deposited or removed between different time periods.

Mercury volume and mass calculations

An estimate of the mass load of mercury within the lower Yuba Fan (**Figure 1**) was calculated from the volume and median mercury concentration of the HMS. For this calculation, we employed the HMS volume (V) computed by the cut-and-fill operation for the period 1852 and 1999, and the average bulk density of the soil found in the lower Yuba Fan (ρ) to determine the mass (M_{fan}) of the lower Yuba Fan (Equation 1). The average bulk density of 1.57×10^3 kg/m^3 was found using the online GIS map from Web Soil Survey (2013). The standard deviation of the bulk density data set was ±0.07 kg/m^3.

$$V\,(m^3) \times \rho\,\left(kg/m^3\right) = M_{fan}\,(kg) \qquad (1)$$

The measured grain size distribution was used to calculate the median sand and fine-grained fractions. The median sand and fine-grained fractions (F) were then used to calculate the mass of the sand and fine-grained sediment within the lower Yuba Fan (M_{sf}) (Equation 2). The gravel fraction was not included in this analysis since the mercury concentration in gravel is zero (Hg does not bond well to gravel clasts due to low surface area to volume ratio).

$$M_{fan}\,(kg) \times F = M_{sf}\,(kg) \qquad (2)$$

The mass of the specified grain sizes (sand and fines) and mercury concentrations within the sand and fine-grained material (C) were used to calculate the mass of the mercury adsorbed by the respective grain sizes (M_{Hg}) (Equation 3). The mercury concentration data reported here are for the fine-grained fraction of the HMS only. We used the median mercury concentration of the sand fraction of the HMS in the Yuba Goldfields of 0.0175 ppm (1.75×10^{-8} kg Hg/kg HMS), reported by Hunerlach (2004) to calculate the amount of mercury in the sand fraction. The interquartile range of the Hunerlach (2004) dataset was 6.6×10^{-9} kg Hg/kg HMS.

$$M_{sf}\,(kg) \times C\,\left(kg\,Hg/kg\,HMS\right) = M_{Hg}\,(g) \qquad (3)$$

The masses of the mercury adsorbed to the sand and fine-grained sediment were then added together to determine the total mass of mercury within the lower Yuba Fan.

Error analysis

The amount of uncertainty in the calculations of the volume of the lower Yuba Fan and the mass load of the mercury within the fan were assessed using standard error propagation calculations. Equation 1 was used to deter-

mine the uncertainty in calculated values (δq) that were the sum of two variables (x and y) with individual errors associated them (δx and δy).For calculations using average or median values, standard deviation and interquartile ranges were used, respectively, as the errors associated with the values.

$$\delta q = \pm \sqrt{(\delta x)^2 + (\delta y)^2} \qquad (4)$$

For operations that used multiplication, Equation 5 was used to determine the propagated error where q is the product of the two variables.

$$\delta q = \pm q \sqrt{(\delta x / x)^2 + (\delta y / y)^2} \qquad (5)$$

Results

Grain size distributions
Figure 4 shows the grain size distribution results plotted on Shepard's classification ternary diagrams (Shepard, 1954; Schlee, 1973). The outcrop samples have similar sediment classification to the boring samples except that they do not contain significant silt or clay fractions. The samples collected from Rose Bar and the Blue Point Mine contained high percentages of gravel.

Mercury concentrations
Figure 5 presents the assay results for all the sediment samples. The total mercury concentrations of the fine-grained fractions of the sediment samples (<63 μm) ranged from order 10^{-2} to 10^0 ppm (mass fraction). The identification numbers of the outcrop samples decrease with increasing depth from the surface corresponding to measurements starting from the bottom of each stratigraphic column. The mercury concentrations of the in situ Tertiary sediment collected from Blue Point Mine (**Figure 6**) are relatively low, of order 10^{-2} ppm, whereas Rose Bar samples of un-reworked (primary) HMS have mercury concentrations predominantly of order 10^0 ppm.

Chemostratigraphy
The samples collected at the Blue Point Mine provide the mercury concentration of native auriferous gravels before being processed with mercury during mining operations.

The mercury concentrations range from 0.017 to 0.056 ppm (**Figure 6**). These concentration values are similar to the average global crustal abundance of mercury of 0.067 ppm (Cox, 1989) and pre-mining sediment concentration levels of 0.02 and 0.05 ppm measured within the lower Yuba Fan (James et al., 2009).

The sediment within fluvial terraces at Rose Bar provides the mercury concentration of primary mining sediment directly after introduction of mercury (**Figure 3**). Field observations suggested that sample R4N was not HMS because it was collected below the stratigraphic contact between the mine tailings (upper unit) and the native soil (lower unit). This was confirmed by the sample's relatively low mercury concentration of 0.035 ppm. For the rest of the samples, the mercury concentrations of the Rose Bar sediment ranges from 1.390 to 10.380 ppm (**Figure 6**). The two orders-of-magnitude difference between the Blue Point Mine and Rose Bar samples confirms that high concentrations of mercury remained within the mining sediment after the amalgamation process, suggesting the likely source of contamination observed along the Yuba farther downstream.

The chemostratigraphy of each boring and outcrop along the lower Yuba Fan was evaluated to determine if the contact between the HMS and pre-mining deposits was reached (**Tables 1** and **2**). Samples consisting of pre-mining sediment are inferred to have mercury concentrations comparable to the samples collected at the Blue Point Mine (order 10^{-2} ppm, **Figure 6**).

The contact between the pre-mining sediment and HMS was found in 5 borings and 4 outcrops (**Tables 1** and **2**). Contacts within the outcrops are generally abrupt except for a gradational contact found within OC6. The grain size distribution analysis showed that the median sand size fraction of all HMS samples was 82% ± 19% (by weight), while the median fine-grained size fraction for HMS samples was 8.7% ± 21%. The median concentration of Hg (kg of Hg per kg of sediment) within the fine-grained fraction was 4.33×10^{-7} kg Hg/kg HMS ± 1.19×10^{-7} kg Hg/kg HMS (0.433 ppm ±0.119). The majority of the HMS samples have light to pale shades of brown and gray (**Table 3**), while the pre-mining sediment samples are mainly darker shades of brown. Darker shades of brown are highly
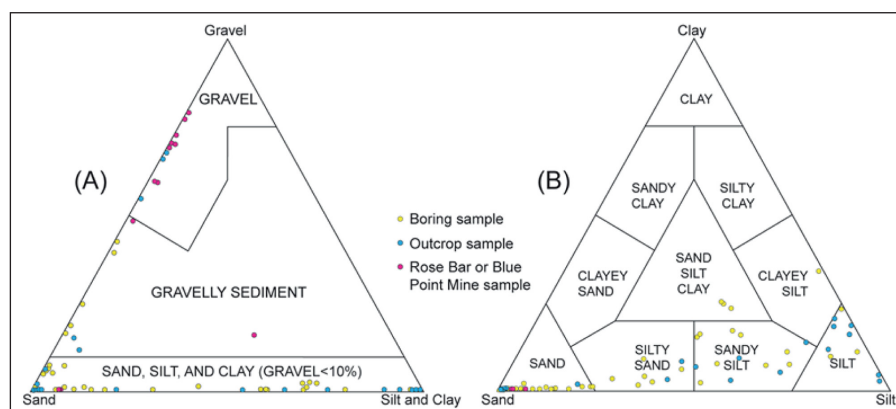

Figure 4: Shepard classification ternary diagrams.Ternary diagram A contains all of the sediment samples with an emphasis on samples with more than 10 percent gravel. Ternary diagram B includes only samples with less than 10 percent gravel. DOI: https://doi.org/10.1525/elementa.333.f4
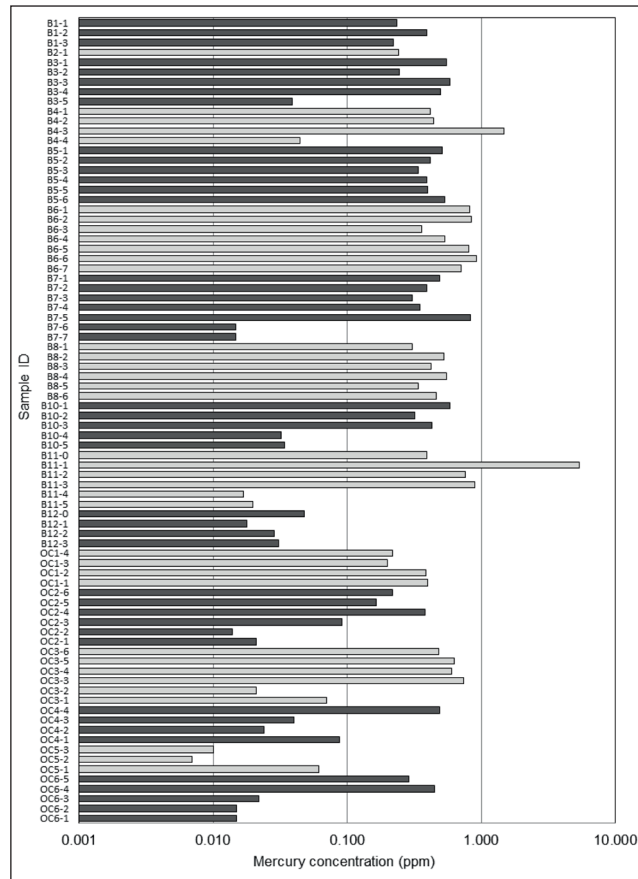
Figure 5: Boring and outcrop sample concentrations in parts per million. DOI: https://doi.org/10.1525/elementa.333.f5
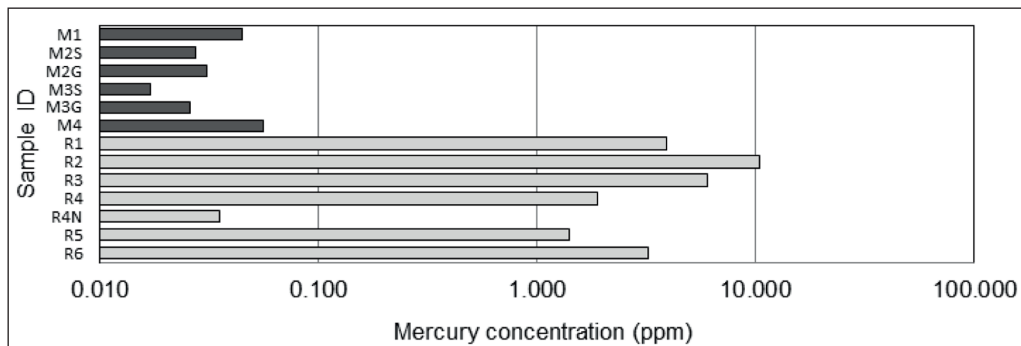
Figure 6: Blue Point Mine and Rose Bar sample mercury concentrations in parts per million. DOI: https://doi.org/10.1525/elementa.333.f6

indicative of the pre-mining sediment while lighter shades of gray and brown are associated with the HMS. Samples within borings B5, B6, B8, and B12 consisted entirely of HMS. Therefore, we assumed that the contact between the HMS and pre-mining deposits was located at the lowest sampling elevation within the boreholes. All of the OC5 outcrop consisted of pre-mining deposits. The contact elevation within the vicinity of the OC5 outcrop was estimated to be located at the highest sampling elevation within the stratigraphic column (**Table 2** and Table S5).

Geomorphic change
Digital elevation models of the surface of the lower Yuba Fan are shown for the following years: 1852, 1911, 1952, and 1999 (**Figure 7**). Table S4 displays the elevations of the pre-mining surface-HMS contact calculated from

these DEMs. The 1852 DEM represents the pre-mining surface of the lower Yuba Fan because that was the year in which major hydraulic mining operations began in the Yuba River watershed.

The amount of elevation change between the DEMs is represented with choropleth maps (**Figure 8**). The maps show elevation differences for four different time intervals: 1852–1911, 1911–1952, 1952–1999, and 1852–1999. Between 1852 and 1911, the minimums amounts of deposition and erosion were 8.0 m and 2.4 m respectively. During the time period between 1911 and 1952, 3.3 m of deposition and up to 9.1 m of incision occurred. We found a maximum of 9.2 m of deposition had occurred during the period between 1952 and 1999. The difference map also shows that up to 9.4 m of erosion occurred from 1952 and 1999. The final difference map

Table 1: Boring chemostratigraphy analysis results. DOI: https://doi.org/10.1525/elementa.333.t1

Sample ID	Depth (m)	Sediment classification	Mercury concentration (parts per million)	Contact depth (m)
B1-1	0.15	Gravelly sediment	0.234	
B1-2	0.40	Gravelly sediment	0.393	Not reached
B1-3	0.52	Sandy silt	0.222	
B2-1	0.15	Sand	0.240	Not reached
B3-1	0.35	Sand	0.553	
B3-2	0.66	Gravelly sediment	0.243	
B3-3	0.84	Sandy silt	0.586	
B3-4	1.16	Sand	0.497	
B3-5	1.51	Sand silt slay	**0.039**[a]	1.32
B4-1	0.40	Gravelly sediment	0.416	
B4-2	0.86	Gravelly sediment	0.438	
B4-3	1.37	Sand	1.470	
B4-4	1.95	Sandy silt	**0.045**	1.85
B5-1	0.71	Sand	0.509	
B5-2	1.40	Sand	0.414	
B5-3	1.83	Sandy silt	0.337	
B5-4	2.70	Silt	0.393	Not reached
B5-5	3.28	Sand	0.396	
B5-6	4.35	Silty sand	0.531	
B6-1	0.48	Sand	0.818	
B6-2	1.50	Sand	0.835	
B6-3	2.52	Silty sand	0.359	
B6-4	3.50	Sand	0.537	Water table encountered at 5.75 m, contact not reached
B6-5	4.50	Silty sand	0.808	
B6-6	5.60	Sand	0.923	
B6-7	5.90	Sandy silt	0.708	
B7-1	0.14	Silty sand	0.488	
B7-2	0.60	Silt	0.389	
B7-3	1.57	Clayey silt	0.305	
B7-4	2.48	Silt	0.351	
B7-5	2.66	Sand	0.830	
B7-6	3.10	Sandy silt	**0.015**	2.80
B7-7	4.08	Silty sand	**0.015**	
B8-1	0.57	Sand	0.307	
B8-2	1.66	Sand	0.525	
B8-3	2.56	Sand	0.419	
B8-4	3.63	Sand	0.551	Not reached
B8-5	4.60	Sand	0.336	
B8-6	5.43	Sand	0.461	
B10-1	0.74	Sand	0.584	
B10-2	1.12	Sand	0.316	

(Contd.)

Sample ID	Depth (m)	Sediment classification	Mercury concentration (parts per million)	Contact depth (m)
B10-3	2.45	Sand	0.429	3.14
B10-4	3.40	Sand silt clay	**0.032**	
B10-5	3.56	Sand silt clay	**0.034**	
B11-0	0.60	Sand	0.393	
B11-1	2.40	Sand	5.362	
B11-2	3.35	Sand	0.759	
B11-3	4.37	Sandy silt	0.892	5.45
B11-4	5.75	Silty sand	**0.017**	
B11-5	6.47	Silty sand	**0.020**	
B12-0	0.00	Sand	**0.048**	
B12-1	0.10	Sand	**0.018**	Not reached
B12-2	0.40	Sandy silt	**0.028**	
B12-3	0.60	Sandy silt	**0.031**	

[a] The bold mercury concentration values indicate pre-mining sediment mercury concentrations.

shows that between 1852 and 1999 there was up to 9.1 m of deposition and 11.9 m of surface erosion (excluding the landfill area).

Cross sections across the fan (**Figure 2**) were created from the DEMs (**Figure 9**) to indicate how the morphological changes were distributed across the fan. Each cross section contains the surface profiles for the years 1852, 1911, 1952, and 1999. The cross sections show the changes in elevation that occurred along each transect since 1852.

Total changes in sediment volume for the same time periods as above are shown in **Figure 10** and are contained in **Table 4**. The results of net volumetric change for the lower Yuba River Fan are as follows: approximately 8.3×10^7 m³ of material was deposited from 1852 to 1911, comprising ~32% of Gilbert's estimate for the entire Yuba Fan deposit (Gilbert, 1917). Between 1911 and 1952, 8.8×10^6 m³ of material was eroded from the lower Yuba Fan, associated with cessation of mining and reworking of HMS. Between 1952 and 1999, 7.0×10^6 m³ of material was deposited, consistent with redistribution of mining sediment from the upper fan to the lower fan (Singer et al., 2013). The total net change (sum of the 1852 to 1911, 1911 to 1952, and 1952 to 1999 cut-and-fill analyses) was 8.1×10^7 m³ of deposited material. The cut-and-fill analysis results between the 1852 and 1999 DEMs also show 8.1×10^7 m³ of deposited material (**Table 4**).

Mercury mass calculations

The results of calculations with Equation 1 showed that the total mass of the HMS within the lower Yuba Fan is 1.3×10^{11} kg. The mass of the HMS was divided by grain size fraction (Equation 2), which resulted in 1.1×10^{11} kg of sand and 1.1×10^{10} kg of fine grained sediment. The mass of mercury within the sand and fine-grained sediment calculated from Equation 3 were 1.9×10^3 kg Hg and 4.8×10^3 kg Hg respectively. The final results of the calculations suggest that approximately 6.7×10^3 kg $\pm 1.2 \times 10^4$ kg of mercury is adsorbed onto the HMS of the lower Yuba

Fan. This estimate of Hg mass is ~3 orders of magnitude smaller than the total estimate of Hg lost to the hydraulic mining process (Alpers and Hunerlach, 2000).

Discussion

This study builds on previous research in this region focused on the legacy 19th Century hydraulic gold mining in the Sierra Nevada foothills by estimating the volume of total HMS storage in the lower Yuba Fan and its associated mercury concentrations at various depths. The new analyses enabled an estimate of total mercury mass stored in the lower Yuba Fan, which may subsequently contribute to contaminant export to the sensitive lowlands of the Sacramento Valley (Singer et al., 2013; Kilham et al., 2012). Distinguishing between HMS and non-HMS in this region was possible using total mercury concentrations in fine sediments as a proxy, which improves on past efforts that used quartz pebble concentrations (James, 1991). The fine-grained (<63 μm) fraction of sediment samples from Rose Bar had mercury concentrations ranging from 1.390 to 10.380 ppm. These concentrations are 2–3 orders of magnitude higher than the Hg concentrations of the pre-mining sediment at the Blue Point Mine. Placer deposits mined and processed at Blue Point Mine and other mines upstream were contaminated with mercury during the amalgamation process and then transported into the Yuba River, where the mine tailings filled narrow sections of the Yuba River valley and built the ~40 km, steep Yuba Fan (**Figure 1**). Following the cessation of mining, the Yuba River re-trenched into these deposits, forming terraces along the Yuba River in the vicinity of Rose Bar and progressively farther downstream. Since the sediment in the Rose Bar terraces emerged directly from the Blue Point Mine, Hg concentrations are high. However, as these sediments are eroded during large floods (Kilham et al., 2012; Singer et al., 2013; Higson and Singer, 2015), the sediment with high mercury concentration becomes diluted with less contaminated sediment, such that new deposits of this

Table 2: Outcrop chemostratigraphy analysis results. DOI: https://doi.org/10.1525/elementa.333.t2

Sample ID	Depth (m)	Sediment classification	Mercury concentration (parts per million)	Contact depth (m)
OC1-4	2.10	Sand	0.217	
OC1-3	3.78	Sand	0.199	7.00
OC1-2	5.51	Gravelly sediment	0.387	(James et al. 2009)
OC1-1	7.13	Gravelly sediment	0.397	
OC2-6	1.64	Sandy silt	0.217	
OC2-5	3.20	Sandy silt	0.164	
OC2-4	3.81	Silty sand	0.381	
OC2-3	4.42	Sandy silt	**0.091**[a]	4.02
OC2-2	5.64	Silty sand	**0.014**	
OC2-1	6.25	Gravel	**0.021**	
OC3-6	2.50	Silt	0.484	
OC3-5	3.57	Sand	0.625	
OC3-4	5.40	Sand	0.601	
OC3-3	7.20	Silt	0.736	
OC3-2	7.74	Sandy silt	**0.021**	7.53
OC3-1	8.45	Gravel	**0.070**	
OC4-4	4.60	Sand	0.489	
OC4-3	7.40	Silt	**0.040**	6.81
OC4-2	9.57	Sand	**0.024**	
OC4-1	11.15	Sand	**0.088**	
OC5-3	2.22	Silt	**0.010**	
OC5-2	4.05	Sandy silt	**0.007**	Not reached
OC5-1	6.49	Gravel	**0.061**	
OC6-5	0.61	Sand	0.289	
OC6-4	3.20	Sand	0.446	
OC6-3	6.40	Silt	**0.022**	5.63
OC6-2	8.17	Silt	**0.015**	
OC6-1	9.51	Silt	**0.015**	

[a] The bold mercury concentration values indicate pre-mining sediment mercury concentrations.

remobilized primary sediment have concentrations that are only one order of magnitude higher than background levels. This downstream pattern continues with subsequent remobilization, whereby Hg concentrations in HMS decrease to 3 times above background levels (Singer et al., 2013).

The chemostratigraphy within the boreholes and outcrops in the lower Yuba Fan provide useful information about the history of HMS storage and remobilization. They reveal abrupt increases in mercury concentrations marking the contact between the pre-mining sediment and the HMS and therefore provide point estimates of the thickness of net HMS accumulation. The sediment near this contact generally consists of sandy HMS overlying relatively fine-grained pre-mining sediment (**Tables 1** and **2**). The contact depth ranges from 1.32 to 7.53 m, based on our borings and outcrop measurements, and the thickness of the deposits

at the sampling sites close to the levees is significantly less than the sampling sites near the modern channel (Table S4 and **Figure 2**). This pattern suggests that HMS deposition contemporaneous with 19th Century mining, and even during recent floods, originates from high sediment concentrations in the Yuba River, followed by overbank flooding and deposition that decants sandy material rapidly from the flow near the channel margins. However, the lower Yuba Fan contains a more complex history of such deposition due to the rapid channel shifting that occurred during and after the mining period (James et al., 2009), yielding a palimpsest of HMS deposition across the fan.

The pre-mining surface that we modeled using ArcGIS had relatively smooth topography compared to the more complex 1911, 1952, and 1999 surfaces (**Figures 9–11**). This was because of the small number of input points

Table 3: Sediment and color classification statistics for HMS and pre-mining sediment. DOI: https://doi.org/10.1525/elementa.333.t3

Hydraulic Mining Sediment		
Shepard sediment classification	**Count**	**Percent**
Sand	31	55%
Gravelly Sediment	7	13%
Sandy Silt	7	13%
Silt	5	9%
Silty Sand	5	9%
Clayey Silt	1	2%
Munsell Color classification	**Count**	**Percent**
Pale Brown or Very Pale Brown	31	55%
Light Yellowish Brown, Light Brownish Gray, or Light Gray	20	36%
Brown or Yellowish Brown	5	9%
Pre-mining Sediment		
Shepard sediment classification	**Count**	**Percent**
Sandy Silt	7	27%
Silt	5	19%
Silty Sand	4	15%
Sand	4	15%
Sand Silt Clay	3	12%
Gravel	3	12%
Munsell color classification	**Count**	**Percent**
Brown, Yellowish Brown, or Grayish Brown	15	58%
Dark Grayish Brown or Dark Yellowish Brown	4	15%
Pale Brown	4	15%
Light Gray	3	12%

used for the surface interpolation. The use of the elevation of the lowest sample in the borings where only HMS was found was a way of assigning the maximum elevation of the contact between the pre-mining sediment and HMS for the surface interpolation (**Table 1**). This was also true for the use of the elevation of the uppermost sample in OC5, which consisted entirely of pre-mining sediment (**Table 2**). Providing maximum elevations of the contact between the pre-mining sediment and HMS at these locations resulted in a minimum volume when calculating the total net change in volume between the 1852 and 1911 surfaces and the 1852 and 1999 surfaces.

From 1852 to 1911, deposition occurred throughout most of the lower Yuba Fan (**Figures 8** and **10**). Accumulation of material was focused towards the center of the fan where the amount of deposition reached a maximum of ~8.1 m (**Figure 8**). Additionally, the total volume of material increased by 8.3×10^7 m³ between 1852 and 1911 (**Figure 10** and **Table 4**), representing the arrival of HMS contemporaneous with active mining and subsequent river avulsions (James et al., 2009).

Comparison between the 1911 and 1952 DEM elevations shows that the lower Yuba Fan was mainly eroded during this time period (**Figures 8** and **10**). The surface elevation decreased by up to 9.1 m, and the volume decreased (slightly) by 8.8×10^6 m³, suggesting export of a small fraction (10%) of the total deposit, focused in the area of the present-day channel as it progressively incised to its modern position (**Figures 8** and **9**). This pattern of localized erosion also occurred within the present-day floodplain, where high-water channels began to solidify their positions (James et al., 2009).

From 1952 to 1999, the elevation of the surface of the lower Yuba Fan decreased in some areas by up to 9.4 m and increased in other areas by up to 9.2 m (**Figure 8**), suggesting a more complex pattern of fan evolution resulting in net accumulation of 7.0×10^6 m³ (**Figure 10**). Channel incision within the central portion of the fan appears to have been the main process of erosion (**Figure 9**), which is consistent with the small amounts of deposition on banks and within floodplains along the Yuba River channel (**Figure 8**). By this time, the Yuba River had become stable at its current location and high-water channels became less numerous.

Over the time period addressed here (1852–1999), we estimate that approximately 8.1×10^7 m³ of HMS was deposited within the study area (**Table 4** and **Figure 10**). Gilbert (1917) estimated that the hydraulic mines within
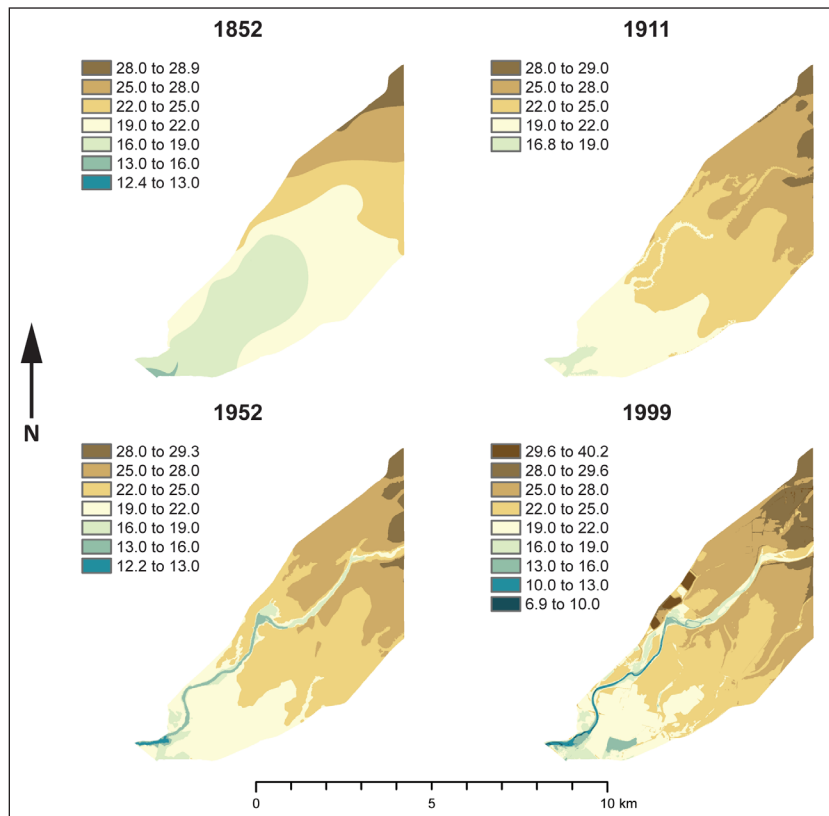
Figure 7: Digital elevation models of the lower Yuba Fan at four points in time. Each DEM has a color ramp displaying the elevation range in meters. DOI: https://doi.org/10.1525/elementa.333.f7
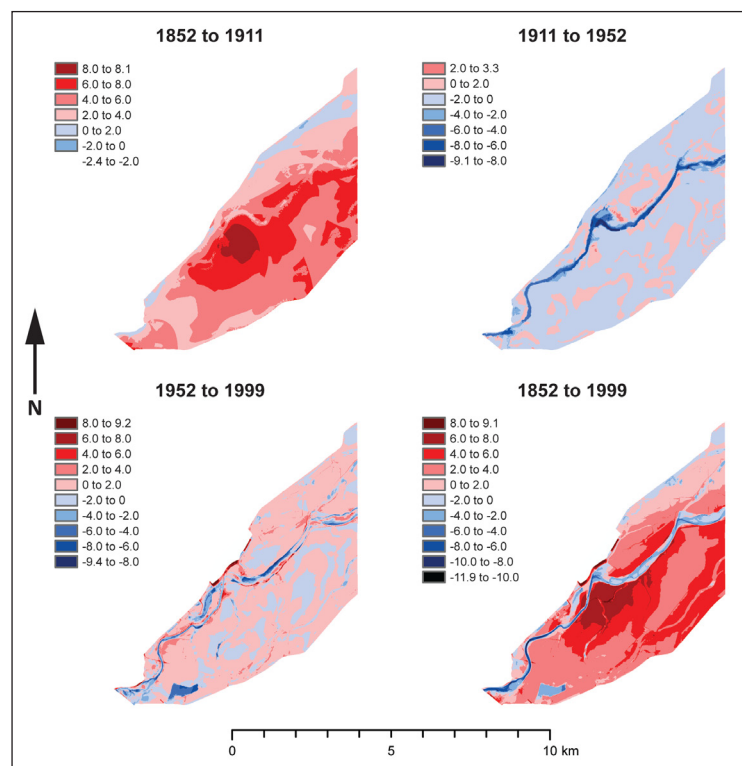

Figure 8: Elevation difference maps for specified time intervals. Each difference map has a color ramp displaying the elevation change in meters. The difference map that displays changes in elevation between 1952 and 1999 shows that there were areas where the elevation increased by up to 9.2 m and decreased by 9.4 m. These areas appear as thin strips of anomalously high elevation increases and decreases along the central portion of the map and are likely due to imprecision in the location of the channel. In terms of the change in volume, the strips of increases and decreases likely offset each other. DOI: https://doi.org/10.1525/elementa.333.f8
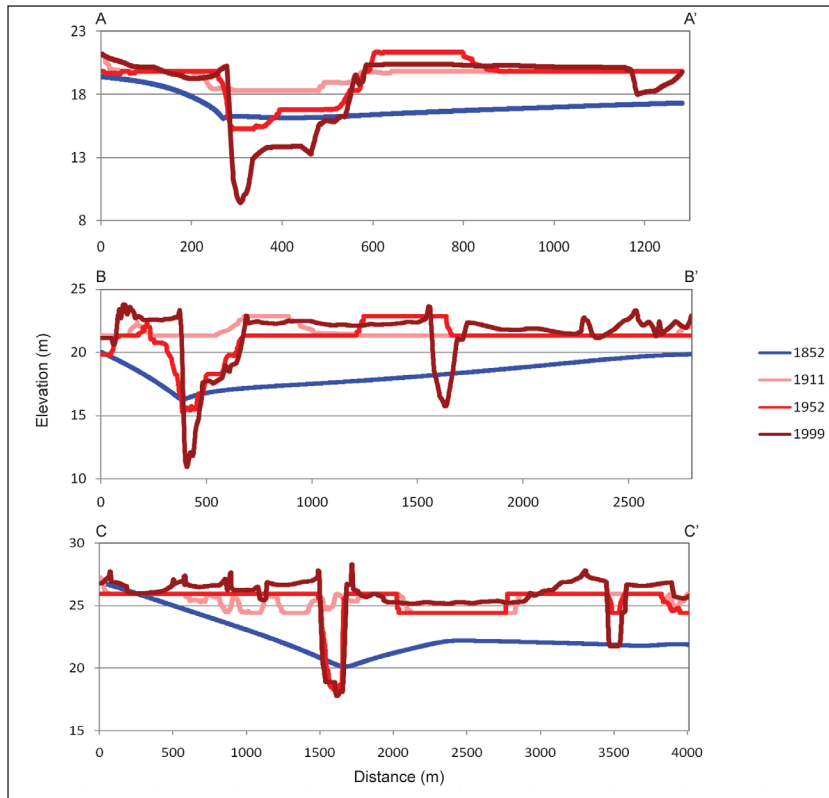
Figure 9: Cross sections A to A', B to B', and C to C'. Each cross section displays the changes in elevation over time. DOI: https://doi.org/10.1525/elementa.333.f9
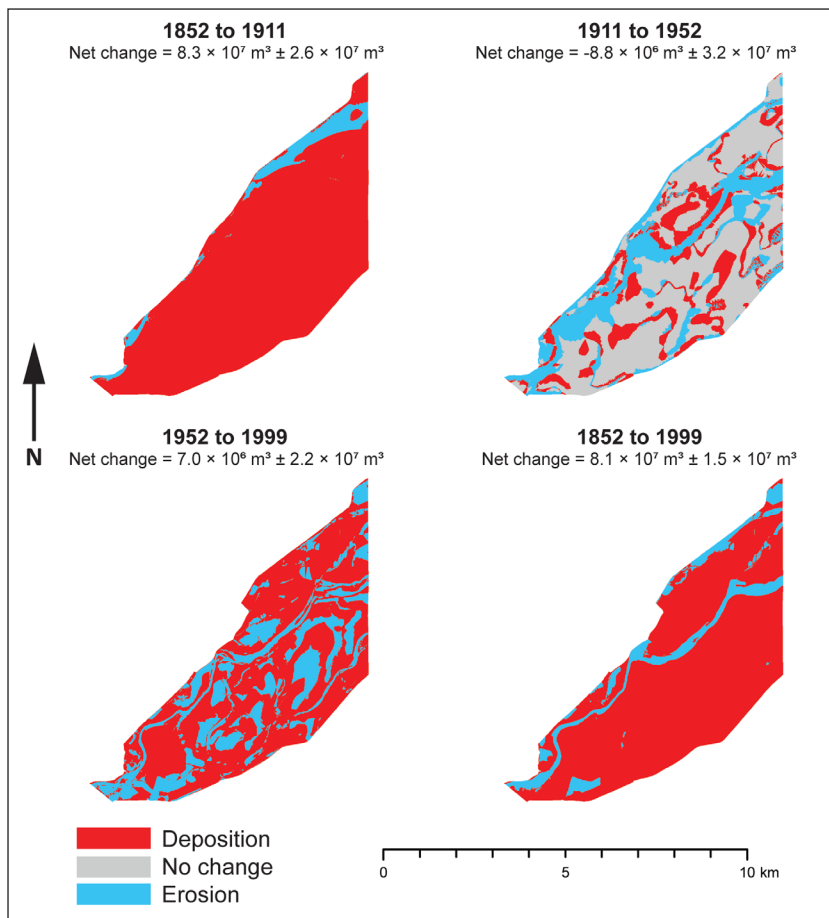

Figure 10: Maps showing areas of deposition and erosion during specified time intervals. The net change in sediment volume is included with each map. DOI: https://doi.org/10.1525/elementa.333.f10

Table 4: Summary of the cut-and-fill operation results. DOI: https://doi.org/10.1525/elementa.333.t4

Time interval	Deposited material (m³)	Eroded material (m³)	Net change (m³)	Accuracy (m³)
1852 to 1911	8.4×10^7	9.2×10^5	8.3×10^7	$\pm 2.6 \times 10^7$
1911 to 1952	5.2×10^6	1.4×10^7	-8.8×10^6	$\pm 3.2 \times 10^7$
1952 to 1999	1.7×10^7	1.0×10^7	7.0×10^6	$\pm 2.2 \times 10^7$
Sum of net changes from 1852 to 1999	–	–	8.1×10^7	$\pm 4.6 \times 10^7$
1852 to 1999	8.8×10^7	7.5×10^6	8.1×10^7	$\pm 1.5 \times 10^7$

the Yuba River watershed produced 5.23×10^8 m³ of HMS between 1849 and 1908. Therefore, based on the work presented here, approximately 15% of Gilbert's estimate of the HMS produced in mines along the Yuba River was deposited in our study area to create the lower Yuba Fan. Gilbert's (1917) estimate of the volume of the entire Yuba Fan was 2.52×10^8 m³ of HMS, but his estimate included the stretch of the fan upstream of our study area from the Yuba Goldfields to the Narrows (**Figure 1**). Attempting to reconcile these two estimates, it appears that the lower Yuba Fan still retains 32% of the original total HMS deposit generated by 19th Century hydraulic mining. We caution that these results should be considered as an approximation, since there are many sources of information with differing resolution and we compared our resulting estimate with that of one calculated by Gilbert.

The mercury concentrations contained in the HMS of the lower Yuba Fan reveal the ongoing contaminant risk to sensitive lowland ecosystems. We estimate a present-day total mercury mass of 6.7×10^3 kg within the lower Yuba Fan. Churchill (1999) determined that, within all the hydraulic gold mines in the Sierra Nevada from the mid-1800s to the early 1900s, 1.4×10^6 to 3.6×10^6 kg of mercury were lost to the environment. Therefore, our results suggest that ~0.2–0.5% of the mercury lost when the hydraulic mines were active in the Sierra Nevada is still stored within the lower Yuba Fan. The large mismatch between these two estimates of mercury mass (total loss versus storage in the lower Yuba Fan) deserves further discussion. There are several possible explanations for the discrepancy. First, the Churchill (1999) estimates of loss during mining processes may be too high due to a misunderstanding of recovery rates, a loss to gaseous phases of mercury, or both. Second, most of the mercury may have already passed through the lower Yuba Fan into the lowlands and into the San Francisco Bay-Delta estuary (Bouse et al., 2001), where it can harm riparian and aquatic ecosystems (Greenfield et al., 2013; Ackerman et al., 2015; Eagles-Smith et al., 2009). Third, our sampling (boring and outcrop locations) may have been biased toward areas of disproportionately low mercury concentrations. Fourth, there may be large pools of mercury stored at unsampled locations within the Yuba River basin that account for the missing Hg mass. Finally, it is also possible that some combination of all four of these factors has resulted in a lower average concentration and total mass of Hg storage in the lower Yuba Fan than was expected based on high estimates of loss during 19th Century gold

mining. On balance, we speculate that the hierarchy of importance of these explanations is 4, 2, 1, and finally 3.

In previous work, Singer et al. (2013) presented a wide range of Hg concentrations with Yuba Fan sediments in outcrops (bank exposures and terraces) and in channel sediments spanning the entire Yuba Fan. These data suggest there is no strong sampling bias toward areas of low Hg concentration within the Fan. Furthermore, in situ Hg degradation is likely to be very low (evidenced by the presence of sediments with a large range of Hg concentrations centuries after deposition), so we did not list this as a possible explanation for the missing Hg. In any case, this mismatch suggests the need for further research to locate the missing mercury in the Yuba basin and other major gold mining drainages in the region, especially given the relevance to the large, important downstream ecosystems and the sizable human population of the region.

Conclusion

The large quantity of HMS deposited along the floodplains of the southern portion of the Yuba River highlights the enduring legacy of hydraulic gold mining operations within the region. Sediment samples were collected from various boreholes and outcrops along the lower Yuba Fan to quantify the amount of HMS accumulated in this area since the onset of 19th Century hydraulic mining operations within the Yuba River watershed. This study revealed that the majority of the HMS was deposited between 1852 and 1911, causing a geomorphic shift from a single channel to a braided river system characterized by thick deposits near the active channel that taper into the adjoining floodplain. After cessation of mining, the HMS supply to the river system decreased, but the geomorphic transformations continued throughout the 20th century, characterized by incision into the original deposit of HMS and net redistribution from upstream to downstream. Quantification of the remaining deposit in the lower Yuba Fan revealed that ~32% of the original deposit (estimated by Gilbert) remains in storage in its lower section. We identified a significant mercury mass stored within this deposit that is available for downstream delivery to sensitive ecosystems, but which is significantly lower than total estimates for mercury loss during the mining process.

Data Accessibility Statement

All data used to develop the figures in this paper are contained within the tables provided and in the supplemental material. The following datasets were generated:

a) boring chemostratigraphy (Table 1)
b) outcrop mercury concentrations (Table 2)
c) sediment grain size and classification (Table 3)
d) averaged volumes of erosion/deposition for the Lower Yuba Fan over different time periods (Table 4)
e) borehole locations, depths, sampling dates, and contact depths (Tables S1–S5)

Supplemental Files

The supplemental files for this article can be found as follows:

- **Table S1.** Borehole site specifications. DOI: https://doi.org/10.1525/elementa.333.s1
- **Table S2.** Outcrop site specifications. DOI: https://doi.org/10.1525/elementa.333.s1
- **Table S3.** Rose Bar and Blue Point Mine site specifications. DOI: https://doi.org/10.1525/elementa.333.s1
- **Table S4.** Contact elevation data for boring and outcrop samples. DOI: https://doi.org/10.1525/elementa.333.s1
- **Table S5.** Contact elevation estimations for field sites where the contact between the pre-mining sediment and HMS was not encountered. DOI: https://doi.org/10.1525/elementa.333.s1

Competing interests

The authors have no competing interests to declare.

Author contributions

Contributed to conception and design of the research: TKN, MBS, EJG. Contributed to analysis and interpretation of data: TKN. Drafted and/or revised the article: TKN, MBS, EJG.

References

Alpers, CN and **Hunerlach, MP.** 2000. Mercury Contamination from Historic Gold Mining in California. *U.S. Geological Survey Fact Sheet 061-00.*

Averill, CV. 1946. Placer mining for gold in California. California State Division of Mines and Geology Bulletin, 135.

Bouse, RM, Fuller, CC, Luoma, S, Hornberger, MI, Jaffe, BE and **Smith, RE.** 2010. Mercury-contaminated Hydraulic Mining Debris in San Francisco Bay. *San Francisco Estuary and Watershed Science Journal* **8**(1).

Bowie, AJ. 1893. A practical treatise on hydraulic mining in California. New York: D. Van Nostrand.

Churchill, R. 1999. Insights into California Mercury Production and Mercury availability for the Gold Mining Industry from the Historical Record. *Geological Society of America Abstracts with Programs* **31**(6).

Cox, PA. 1989. The Elements: Their Origin, Abundance, and Distribution. Oxford, UK: Oxford University Press.

Cristol, DA, Brasso, RL, Condon, AM, Fovargue, RE, Friedman, SL, Hallinger, KK, Monroe, AP and **White, AE.** 2008. The Movement of Aquatic Mercury Through Terrestrial Food Webs. *Science* **320**(5874). DOI: https://doi.org/10.1126/science.1154082

Davis, JA, Greenfield, BK, Ichikawa, G and **Stephenson, M.** 2008. Mercury in sport fish from the Sacramento-San Joaquin Delta region, California, USA. *Science of the Total Environment* **39**1(1): 66–75. DOI: https://doi.org/10.1016/j.scitotenv.2007.10.050

Donovan, PM, Blum, JD, Singer, MB, Marvin-DiPasquale, M and **Tsui, MTK.** 2016a. Methylmercury Degradation and Exposure Pathways in Streams and Wetlands impacted by Historical Mining. *Science of the Total Environment* **568**: 1192–1203. DOI: https://doi.org/10.1016/j.scitotenv.2016.04.139

Donovan, PM, Blum, JD, Singer, MB, Marvin-DiPasquale, M and **Tsui, MTK.** 2016b. Isotopic Composition of Inorganic Mercury and Methylmercury Downstream of a Historical Gold Mining Region. *Environmental Science and Technology* **50**(4): 1691–1702. DOI: https://doi.org/10.1021/acs.est.5b04413

Environmental Systems Research Institute. 2013. ArcGIS. (10.2). [software]: Redlands California (CD-ROM).

Ghoshal, S, James, LA, Singer, MB and **Aalto, R.** 2010. Channel and Floodplain Change Analysis over a 100-year Period: Lower Yuba River, California. *Remote Sensing*, **2**(7): 1797–1825. DOI: https://doi.org/10.3390/rs2071797

Gilbert, GK. 1917. Hydraulic-Mining Debris in the Sierra Nevada. *U.S. Geological Survey Professional Paper 105.*

Gilmour, CC, Podar, M, Bullock, AL, Graham, AM, Brown, SD, Somenahally, AC, Johs, A, Hurt, RA, Jr., Bailey, KL and **Elias, DA.** 2013. Mercury Methylation by Novel Microorganisms from New Environments. *Environmental Science and Technology* **47**(20): 11810–11820. DOI: https://doi.org/10.1021/es403075t

Heim, WA, Coale, KH, Stephenson, M, Choe, KY, Gill, GA and **Foe, C.** 2007. Spatial and Habitat-Based Variations in Total and Methyl Mercury Concentrations in Surficial Sediments in the San Francisco Bay-Delta. *Environmental Science and Technology* **41**(10): 3501–3507. DOI: https://doi.org/10.1021/es0626483

Henery, RE, Sommer, TR and **Goldman, CR.** 2010. Growth and Methylmercury Accumulation in Juvenile Chinook Salmon in the Sacramento River and Its Floodplain, the Yolo Bypass. *Transactions of the American Fisheries Society* **139**(2): 550–563. DOI: https://doi.org/10.1577/T08-112.1

Higson, J and **Singer, M.** 2015. The Impact of the Streamflow Hydrograph on Sediment Supply from Terrace Erosion. *Geomorphology* **248**: 475–488. DOI: https://doi.org/10.1016/j.geomorph.2015.07.037

Hunerlach, MP, Alpers, CN, Marvin-DiPasquale, M, Taylor, HE and **De Wild, JF.** 2004. Geochemistry of Mercury and other Trace Elements in Fluvial Tailings upstream of Daguerre Point Dam, Yuba River, California, August 2001. *U.S. Geological Survey Scientific Investigations Report 2004-5165.* DOI: https://doi.org/10.3133/sir20045165

Hunerlach, MP, Rytuba, JJ and **Alpers, CN.** 1999. Mercury contamination from hydraulic placer-gold mining in the Dutch Flat mining district, California. In: Morganwalp, DW and Buxton, HT (eds.), *U.S. Geological Survey Toxic Substances Hydrology Program – Proceedings of the Technical Meeting.* Charleston, South Carolina, March 8–12, 1999. U.S. Geological Survey Water-Resources Investigations Report 1999-4018. **B**(2): 179–189

Hutchinson, MF. 1989. A New Procedure for Gridding Elevation and Stream Line Data with Automatic Removal of Spurious Pits. *Journal of Hydrology* **106**(3–4): 211–232. DOI: https://doi.org/10.1016/0022-1694(89)90073-5

James, LA. 1989. Sustained storage and transport of hydraulic gold mining sediment in the Bear River: California. *Annals of the American Association of Geographers* **79**(4): 570–592. DOI: https://doi.org/10.1111/j.1467-8306.1989.tb00277.x

James, LA. 1991. Incision and morphologic evolution of an alluvial channel recovering from hydraulic mining sediment. *GSA Bulletin* **103**(6): 723–736. DOI: https://doi.org/10.1130/0016-7606(1991)103<0723:IAMEOA>2.3.CO;2

James, LA. 1997. Channel incision on the lower American River, California, from streamflow records. *Water Resources Research* **33**(3): 485–490. DOI: https://doi.org/10.1029/96WR03685

James, LA. 2004. Decreasing sediment yields in northern California: Vestiges of hydraulic gold-mining and reservoir trapping. In: *International Association of Hydrological Sciences, Proceedings International Symposium on Sediment Transfer through the Fluvial System* **288**: 235–244. 2–6 August 2004. Wallingford: UK. Moscow, Russia

James, LA. 2005. Sediment from hydraulic mining detained by Englebright and small dams in the Yuba Basin. *Geomorphology* **71**(1–2): 202–226. DOI: https://doi.org/10.1016/j.geomorph.2004.02.016

James, LA, Singer, MB, Ghoshal, S and **Megison, M.** 2009. Historical channel changes in the lower Yuba and Feather Rivers, California: Long-term effects of contrasting river management strategies. *Geological Society of America Special Paper* **451**: 57–81. DOI: https://doi.org/10.1130/2009.2451(04)

Kelley, R. 1998. Battling the Inland Sea. University of California Press.

Kilham, NE, Roberts, D and **Singer, MB.** 2012. Remote Sensing of Suspended Sediment Concentration During Turbid Flood Conditions on the Feather River, California—A Modeling Approach. *Water Resources Research* **48**(1). DOI: https://doi.org/10.1029/2011WR010391

Lindgren, W. 1911. The Tertiary gravels of the Sierra Nevada of California. *U.S. Geological Survey Professional Paper, 73.*

Mergler, D, Anderson, HA, Chan, LHM, Mahaffey, KR, Murray, M, Sakamoto, M and **Stern, AH.** 2007. Methylmercury Exposure and Health Effects in Humans. A Worldwide Concern. *AMBIO: A Journal of the Human Environment* **36**(1): 3–11. DOI: https://doi.org/10.1579/0044-7447(2007)36[3:MEAHEI]2.0.CO;2

Olund, SD, DeWild, JF, Olson, Ml and **Tate, MT.** 2005. Methods for the preparation and Analysis of Solids and Suspended Solids for Total Mercury, Book 5-Laboratory Analysis, Techniques and Methods. Reston, VA: U.S. Geological Survey.

Schlee, J. 1973. Atlantic Continental Shelf and Slope of the United States — Sediment Texture of the Northeastern Part. *U.S. Geological Survey Professional Paper 529-L.*

Shepard, FP. 1954. Nomenclature based on Sand-silt-clay Ratios. *Journal of Sedimentary Petrology* **24**(3): 151–158. DOI: https://doi.org/10.1306/D4269774-2B26-11D7-8648000102C1865D

Singer, MB, Aalto, R and **James, LA.** 2008. Status of the Lower Sacramento Valley flood-Control System within the Context of its Natural Geomorphic Setting. *Natural Hazards Review* **9**(3): 104–115. DOI: https://doi.org/10.1061/(ASCE)1527-6988(2008)9:3(104)

Singer, MB, Aalto, R, James, LA, Kilham, NE, Higson, JL and **Ghoshal, S.** 2013. Enduring Legacy of a Toxic Fan via Episodic Redistribution of California Gold Mining Debris. *Proceedings of the National Academy of Sciences* **110**(46): 18436–18441. DOI: https://doi.org/10.1073/pnas.1302295110

Singer, MB, Harrison, LR, Donovan, PM, Blum, JD and **Marvin-DiPasquale, M.** 2016. Hydrologic Indicators of Hot Spots and Hot Moments of Mercury Methylation Potential along River Corridors. *Science of the Total Environment* **568**: 697–711. DOI: https://doi.org/10.1016/j.scitotenv.2016.03.005

Springborn, M, Singer, MB and **Dunne, T.** 2011. Sediment-adsorbed total mercury flux through Yolo Bypass, the primary floodway and wetland in the Sacramento Valley, California. *Sci. Total Environ* **412–413**: 203–213. DOI: https://doi.org/10.1016/j.scitotenv.2011.10.004

Stonestreet, SE and **Lee, AS.** 2000. Use of LIDAR mapping for floodplain studies, in Building Partnerships. In: American Society of Civil Engineers, *Proceedings of the 2000 Joint Conference on Water Resource Engineering, Planning, and Management.* Minneapolis, MN, 30 July–2 August 2000. Pullman: WA. DOI: https://doi.org/10.1061/40517(2000)58

USDA-FSA-APFO Aerial Photography Field Office. 2014a. FSA 10:1 NAIP Imagery m_3912152_nw_10_1_20140725_20141007 3.75 × 3.75 minute JPEG2000. Available through: U.S. Geological Survey The National Map <https://nationalmap.gov/> [Accessed 10 November 2016].

USDA-FSA-APFO Aerial Photography Field Office. 2014b. FSA 10:1 NAIP Imagery m_3912152_ne_10_1_20140725_20141007 3.75 × 3.75 minute JPEG2000 from The National Map: USDA-FSA-APFO Aerial Photography Field Office.

USDA-FSA-APFO Aerial Photography Field Office. 2014c. FSA 10:1 NAIP Imagery m_3912153_nw_10_1_20140725_20141007 3.75 × 3.75 minute JPEG2000 from The National Map: USDA-FSA-APFO Aerial Photography Field Office.

USDA-FSA-APFO Aerial Photography Field Office. 2014d. FSA 10:1 NAIP Imagery m_3912152_sw_10_1_20140725_20141007 3.75 × 3.75 minute JPEG2000 from The National Map: USDA-FSA-APFO Aerial Photography Field Office.

USDA-FSA-APFO Aerial Photography Field Office. 2014e. FSA 10:1 NAIP Imagery m_3912152_se_10_1_20140725_20141007 3.75 × 3.75 minute JPEG2000 from The National Map: USDA-FSA-APFO Aerial Photography Field Office.

USDA-FSA-APFO Aerial Photography Field Office. 2014f. FSA 10:1 NAIP Imagery m_3912153_sw_10_1_20140725_20141007 3.75 × 3.75 minute JPEG2000 from The National Map: USDA-FSA-APFO Aerial Photography Field Office.

USDA-FSA-APFO Aerial Photography Field Office. 2014g. FSA 10:1 NAIP Imagery m_3912154_ne_10_1_20140713_20141007 3.75 × 3.75 minute JPEG2000 from The National Map: USDA-FSA-APFO Aerial Photography Field Office.

U.S. Geological Survey. 1911. USGS 1:31680-scale Quadrangle for Yuba City, CA 1911 [Topographic Map]. Retrieved from: https://prdtnm.s3.amazonaws.com/StagedProducts/Maps/Historical-Topo/2/13241/4753174.pdf.

U.S. Geological Survey. 1952. USGS 1:24000-scale Quadrangle for Yuba City, CA 1952 [Topographic Map]. Retrieved from: https://prd-tnm.s3.amazonaws.com/StagedProducts/Maps/HistoricalTopo/2/13260/4779554.pdf [Accessed 5 November 2016].

U.S. Geological Survey. 1999. Map Accuracy Standards. *U.S. Geological Survey Fact Sheet*, 171–99.

U.S. Geological Survey. 2013. USGS NED n40w122 1/3 arc-second 2013 1 × 1 degreeArcGrid: U.S. Geological Survey.

Web Soil Survey 3.2. 2013. Natural Resources Conservation Service, United States Department of Agriculture. Lower Yuba Fan Study Area 39°09′02″N, 121°33′11″W, Bulk Density, 1/3 Bar layer. Available through: <http://websoilsurvey.nrcs.usda.gov/> [Accessed 5 November 2016].

Wiener, JG and **Suchanek, TH.** 2008. The Basis for Ecotoxicological Concern in Aquatic Ecosystems Contaminated by Historical Mercury Mining. *Ecological Applications* **18**(8): A3–A11. DOI: https://doi.org/10.1890/06-1939.1

Windham-Myers, L, Fleck, JA, Ackerman, JT, Marvin-DiPasquale, M, Stricker, CA, Heim, WA, Bachand, PAM, Eagles-Smith, CA, Gill, G, Stephenson, M and **Alpers, CN.** 2014. Mercury Cycling in Agricultural and Managed Wetlands: A Synthesis of Methylmercury Production, Hydrologic Export, and Bioaccumulation from an Integrated Field Study. *Science of The Total Environment* **484**: 221–231. DOI: https://doi.org/10.1016/j.scitotenv.2014.01.033

Yeend, WE. 1974. Gold-bearing gravel of the ancestral Yuba River, Sierra Nevada, California. *U.S. Geological Survey Professional Paper 772.*